Supporting Information

for

Magnetic Resonance Imaging of High-Intensity Focused Ultrasound-Stimulated Drug Release from a Self-Reporting Core@Shell Nanoparticle Platform

Chi-An Cheng,[a,d] *Wei Chen,*[b,d] *Le Zhang,*[c] *Holden H. Wu,*[a,c,*] *and Jeffrey I. Zink*[b,d,*]

a Department of Bioengineering, University of California Los Angeles, Los Angeles, California 90095, United States

b Department of Chemistry & Biochemistry, University of California Los Angeles, Los Angeles, California 90095, United States

c Department of Radiological Sciences, David Geffen School of Medicine, University of California Los Angeles, Los Angeles, California 90095, United States

d California NanoSystems Institute, University of California Los Angeles, California 90095, United States

* Corresponding authors: zink@chem.ucla.edu, HoldenWu@mednet.ucla.edu

Table of Contents

I. Materials and general experimental procedures

Materials

Iron(III) acetylacetonate ($Fe(acac)_3$, 97%), manganese(II) acetylacetonate ($Mn(acac)_2$, 21%-23% Mn), cobalt(II) acetylacetonate ($Co(acac)_2$, 97%), 1,2-dodecanediol (90%), oleic acid (90%), oleylamine (70%), benzyl ether (98%), hexane (98.5+%), chloroform (99.5+%), hexadecyltrimethylammonium bromide (CTAB, 99+%), tetraethyl orthosilicate (TEOS, 98%), (3-aminopropyl)triethoxysilane (APTS, 99%), 4,4′-azobis(4-cyanovaleric acid) (ACVA, 98+%) 1-adamantylamine (AMA, 97%), *β*-cyclodextrin (*β*-CD, 97+%), ammonium nitrate (NH_4NO_3, 98+%), 1-Ethyl-3-(-3-dimethylaminopropyl) carbodiimide (EDC, 98+%), *N*-hydroxysuccinimide (NHS, 98%), phosphate-buffered saline (PBS, 10X), and bisBenzimide H 33342 trihydrochloride (Hoechst 33342, 98+%) were purchased from Sigma-Aldrich. Doxorubicin hydrochloride (DOX-HCl) was purchased from Cayman Chemical. Dimethyl sulfoxide (DMSO, 99.9+%), sodium hydroxide (NaOH, 97+%), hydrochloric acid (HCl, 36.5%-38%, tracemetal grade), and nitric acid (HNO_3, 67%-70%, tracemetal grade) were purchased from Fisher Scientific. Dulbecco's modified Eagle's medium (DMEM) with high glucose, fetal bovine serum (FBS), antibiotics (10,000 U/mL penicillin, 10,000 μg/mL streptomycin, and 29.2 mg/mL L-glutamine), Dulbecco's phosphate-buffered saline (DPBS), and trypsin-ethylenediaminetetraacetic acid (trypsin-EDTA) (0.05 %) were purchased from Gibco. Cell counting kit-8 (CCK-8) was purchased from Dojindo Molecular Technologies, Inc. Paraformaldehyde solution (4 % in PBS) was purchased from USB Corporation. Ethanol (200 proof) was purchased from Decon Laboratories, Inc. All chemicals were used without further purification.

Characterization procedures

The morphology and diameters of nanoparticles were investigated by transmission electron microscopy (TEM, Tecnai T12) with an operating voltage of 120 kV. $MnFe_2O_4$@$CoFe_2O_4$ or MNP@MSN core@shell nanoparticles were dispersed in hexane or ethanol at a low concentration (0.2 mg/mL). The suspension (10 μL) of the nanoparticles was dropped onto the carbon-coated copper grid and dried at room temperature. The dynamic light scattering (DLS) size and ζ-potential values of the nanoparticles were determined by a laser particle analyzer LPA-3100 in deionized water at room temperature (24 °C). Thermogravimetric analysis (TGA) was performed on a Perkin-Elmer Pyris Diamond TG/DTA machine under air flow (200 mL/min). MNP@MSNs, MNP@MSNs-APTS, MNP@MSNs-ACVA, and MNP@MSNs-AMA (about 5 mg) were loaded in aluminum pans and the data were recorded from 20 °C to 600 °C at a scan rate of 20 °C/min. The plotted values were normalized to the weight at 100°C. An empty aluminum pan was used as a reference. The functional groups on the surface of MNP@MSNs were characterized by Fourier transform infrared spectroscopy (FTIR, JASCO FT/IR-420) spectrometer in the range of 4000–400 cm^{-1}. The loading capacity and release efficiency of DOX were calculated using the fluorescence intensity integrated from 585 and 595 nm (λ_{ex} = 480 nm) determined by a plate reader (Tecan M1000). The metal ions (Fe, Mn, and Co) concentration of MNP@MSNs-AMA-CD were quantified by inductively coupled plasma optical emission spectrometry (ICP-OES) using a Shimadzu ICPE-9000.

Abbreviations

4,4′-azobis(4-cyanovaleric acid) (ACVA), 1-adamantylamine (AMA), (3-Aminopropyl)triethoxysilane (APTS), *β*-cyclodextrin (*β*-CD), cell counting kit-8 (CCK-8), cobalt(II) acetylacetonate ($Co(acac)_2$), hexadecyltrimethylammonium bromide (CTAB), dynamic light scattering (DLS), Dulbecco's modified Eagle's medium (DMEM), dimethylsulfoxide (DMSO), doxorubicin (DOX), Dulbecco's phosphate-buffered saline (DPBS), 1-ethyl-3-(-3-dimethylaminopropyl) carbodiimide (EDC), fetal bovine serum (FBS), iron(III) acetylacetonate ($Fe(acac)_3$), Fourier-transform infrared spectroscopy (FT-IR), hydrochloric acid (HCl), high-intensity focused ultrasound (HIFU), bisBenzimide H 33342 trihydrochloride (Hoechst 33342), inductively coupled plasma optical emission spectrometry (ICP-OES), manganese(II) acetylacetonate ($Mn(acac)_2$), magnetic resonance imaging-guided high-intensity focused ultrasound (MRgHIFU), magnetic resonance imaging (MRI), mesoporous silica nanoparticles (MSNs), sodium hydroxide (NaOH), ammonium nitrate (NH_4NO_3), *N*-hydroxysuccinimide (NHS), pancreatic cancer cells (PANC-1), phosphate buffer saline (PBS), superparamagnetic iron oxide nanoparticles (SPIONs), transmission electron microscope (TEM), tetraethyl orthosilicate (TEOS), thermogravimetric (TGA), trypsin-ethylenediaminetetraacetic acid (trypsin-EDTA)

Cell culture procedures

Human pancreatic cancer cells (PANC-1) were cultured in T-25 flasks (Corning) with vented caps in a high glucose DMEM supplemented with 10 % FBS, and 1 % antibiotics (100 U/mL penicillin and 100 μg/mL streptomycin) in a humidity-controlled incubator at 37 °C with 5 % CO_2. The PANC-1 culture media were daily changed and the cells were harvested by trypsinization with 0.05 % trypsin-EDTA for passaging every 2-3 days.

Preparation of agarose phantom

In the community of MRI and ultrasound research, it is customary to first use tissue-mimicking phantoms to evaluate feasibility, train operators, optimize protocols, and characterize technical performance of the technology before studying animal or human subjects.[1,2] Tissue-mimicking phantoms use materials designed to mimic pertinent properties of biological tissues, and thus are used in preclinical research as an alternative to *ex vivo* tissues and organs. An agarose gel "phantom" (*i.e.*, test object) was prepared and used as the sample holder for DOX-loaded MNP@MSNs-AMA-CD or cells during MRgHIFU experiments. The concentration of the agarose used was 3.5 wt %. Agarose powder (17.5 g) was added slowly to a 1000 mL flask with deionized H_2O (500 mL) during vigorous stirring. The solution was then heated to boiling and maintained at that temperature for 5 min. Subsequently, the hot solution was poured into a plastic container with a diameter of 10 cm and the sample wells were molded by glass test tubes with a diameter of 1.3 cm. The solution was finally cooled down to 4 °C for the gel formation.

Preparation of methylcellulose gel

To prepare methylcellulose gel (2.5 wt %), methylcellulose powder (1.25 g) was slowly added to 15 mL of boiling water in a flask while vigorous stirring to dissolve the powder. After stirring for 3 min, 35 mL of room temperature water was rapidly added to the solution and mixed homogeneously. The solution was then cooled at 4 °C overnight to complete the gelation process.

T_2 mapping

T_2 maps of water-suspended DOX-loaded MNP@MSNs-AMA-CD before and after the stimulation by a probe sonicator or MRgHIFU were acquired using a 3 T MRI scanner (Prisma, Siemens Healthineers, Erlangen, Germany) with a 2D turbo-spin-echo (TSE) protocol. 1 mL of samples with and without HIFU stimulation were mixed with 3 mL of methylcellulose (2.5 wt %) in 15 mL Falcon plastic tubes placed in a water bath.
Parameters for the T_2 mapping protocol were: 2D multiple-TE TSE sequence; FOV= 350 × 350 mm^3; matrix size= 256 × 256; slice thickness=3 mm; 20 slices; TEs= 12, 24, 35, 47, 59, 83, 94, 118 ms; TR= 8s; excitation pulse flip angle = 90°; refocusing pulse flip angle= 180°. T_2 (ms) was calculated using a mono-exponential fitting algorithm (Note S1).

T_2 relaxivity (r_2) measurement
Different concentrations of DOX-loaded MNP@MSNs-AMA-CD were mixed with 2.5 wt % methylcellulose. T_2 relaxation times were acquired by the 3 T MRI scanner using the above multiple-TE TSE sequence. r_2 ($s^{-1}mM^{-1}$) was calculated as the ratio of $1/T_2$ to the total concentrations of Fe, Mn, and Co as determined by ICP-OES.

II. Experimental procedures

Synthesis of $MnFe_2O_4$@$CoFe_2O_4$ nanoparticles

Synthesis of $MnFe_2O_4$ nanoparticles: $MnFe_2O_4$ nanoparticles were synthesized following a previously reported method with a slight modification.[3,4] Two mmol of $Fe(acac)_3$, 1 mmol of $Mn(acac)_2$, 10 mmol of 1,2-dodecanediol, 6 mmol of oleic acid, and 6 mmol of oleylamine were dissolved in 20 mL of benzyl ether in a three-neck flask. The reaction was heated to 200 °C under the flow of nitrogen with vigorously stirring and kept at that temperature for 1 h. The reaction mixture was then heated up and refluxed for 1 h (298 °C). Afterwards, the resulting solution containing $MnFe_2O_4$ nanoparticles was cooled to room temperature. The nanoparticles were precipitated by adding 40 mL of ethanol and further separated by centrifugation (7830 rpm, 10 min). Finally, $MnFe_2O_4$ nanoparticles were dispersed in 10 mL of hexane with 50 μL of oleic acid and 50 μL of oleylamine. The larger $MnFe_2O_4$ nanoparticles were synthesized by growing $MnFe_2O_4$ on the previously resulted $MnFe_2O_4$ nanoparticles through the similar procedure. Generally, two mmol of $Fe(acac)_3$, 1 mmol of $Mn(acac)_2$, 10 mmol of 1,2-dodecanediol, 2 mmol of oleic acid, and 2 mmol of oleylamine were dissolved in 20 mL of benzyl ether in a 100 mL three-neck flask. The $MnFe_2O_4$ nanoparticles (90 mg) obtained previously in 10 mL of hexane were added to the reaction mixture. The reaction mixture was heated to 90 °C and kept at that temperature for 30 min to remove hexane. Then the reaction mixture was heated to 200 °C under the flow of nitrogen with vigorously stirring. After 1 h, the reaction mixture was heated to 298 °C and refluxed for 1 h. The nanoparticles were precipitated by adding 40 mL of ethanol and further separated by centrifugation. Finally, the $MnFe_2O_4$ nanoparticles were re-dispersed in 10 mL of hexane with 50 μL of oleic acid and 50 μL of oleylamine.

Synthesis of $MnFe_2O_4$@$CoFe_2O_4$ nanoparticles: To coat $CoFe_2O_4$ on the surface of $MnFe_2O_4$ nanoparticles, two mmol of $Fe(acac)_3$, 1 mmol of $Co(acac)_2$, 10 mmol of 1,2-dodecanediol, 2 mmol of oleic acid, and 2 mmol of oleylamine were dissolved in 20 mL of benzyl ether in a 100 mL three-neck flask. The $MnFe_2O_4$ nanoparticles (180 mg) obtained previously in 10 mL of hexane were added to the reaction mixture. The synthetic procedure and reaction temperature were the same as that of the above-mentioned. Finally, $MnFe_2O_4$@$CoFe_2O_4$ nanoparticles were re-dispersed in 10 mL of hexane with 50 μL of oleic acid and 50 μL of oleylamine. To obtain larger $MnFe_2O_4$@$CoFe_2O_4$, another $CoFe_2O_4$ was further coated on the surface of the previously resulted $MnFe_2O_4$@$CoFe_2O_4$ nanoparticles. Two mmol of $Fe(acac)_3$, 1 mmol of $Co(acac)_2$, 10 mmol of 1,2-dodecanediol, 2 mmol of oleic acid, and 2 mmol of oleylamine were dissolved in 20 mL of benzyl ether in a 100 mL three-neck flask. $MnFe_2O_4$@$CoFe_2O_4$ nanoparticles (270 mg) obtained previously in 10 mL of hexane were added to the reaction mixture. The synthetic procedure and reaction temperature were the same as that of the above-mentioned. Finally, $MnFe_2O_4$@$CoFe_2O_4$ nanoparticles (11.0 nm) were re-dispersed in 10 mL of hexane with 50 μL of oleic acid and 50 μL of oleylamine for further use.

Synthesis of APTS functionalized $MnFe_2O_4$@$CoFe_2O_4$@mesoporous silica core@shell nanoparticles (MNP@MSNs-APTS)

$MnFe_2O_4$@$CoFe_2O_4$ nanoparticles (11.0 nm, 2.5 mg) were dispersed in 0.2 mL of chloroform. 2 mL of CTAB aqueous solution (40 mg of CTAB, 54 mM) was added to the $MnFe_2O_4$@$CoFe_2O_4$ colloidal solution, and the mixture was sonicated for 10 min with a fully sealed cover to generate oil-in-water emulsion. The emulsion was then sonicated for 1 h to evaporate chloroform. The clear and well-dispersed $MnFe_2O_4$@$CoFe_2O_4$ colloidal aqueous solution (2 mL) was obtained

(designated as $MnFe_2O_4$@$CoFe_2O_4$@CTAB). Meanwhile, 40 mg of CTAB was dissolved in 18 mL of water with 120 μL of NaOH solution (2 M) in a 100 mL flask. The previously obtained $MnFe_2O_4$@$CoFe_2O_4$@CTAB colloidal solution (2 mL) was added to the reaction solution with vigorously stirring, and the temperature of the solution was brought up to 70 °C. To coat mesoporous silica shell on the surface of $MnFe_2O_4$@$CoFe_2O_4$@CTAB, 200 μL of TEOS and 1.2 mL of ethyl acetate were added dropwise into the solution. After stirring for 2 h, 40 μL of APTS was added dropwise into the solution and stirred for another 2 h. The resulted amine functionalized $MnFe_2O_4$@$CoFe_2O_4$@MSNs was designated as MNP@MSNs-APTS (MNP denotes "magnetic nanoparticle"). Afterwards, the solution was cooled to room temperature and MNP@MSNs-APTS was centrifuged and washed 3 times with ethanol. Subsequently, MNP@MSNs-APTS was dispersed in 20 mL of ethanol containing 120 mg of NH_4NO_3 and the reaction was stirred at 60 °C for 1 h to remove the surfactants. The surfactant removal procedures were repeated twice and MNP@MSNs-APTS was washed several times with deionized water and ethanol to obtain the surfactant-free MNP@MSNs-APTS.

Synthesis of ACVA functionalized MNP@MSNs-APTS (MNP@MSNs-ACVA)

The conjugation of ACVA to the surface of MNP@MSNs-APTS was carried out by using an amide bond coupling reaction (Scheme S1). At first, the carboxylic acid of ACVA (20 mg) was activated by EDC (40 mg) and NHS (20 mg) in DMSO (4 mL). To crosslink the activated ACVA to the primary amine of APTS, after 30 min activation at room temperature, 20 mg of MNP@MSNs-APTS dispersed in DMSO (4 mL) were added dropwise to the activated ACVA in DMSO and stirred for 24 h. The ACVA functionalized MNP@MSNs-APTS (MNP@MSNs-ACVA) was washed, centrifuged, and re-suspended in DMSO three times to remove the excess ACVA, EDC, and NHS.

Synthesis of AMA functionalized MNP@MSNs-ACVA (MNP@MSNs-AMA)

The conjugation of AMA to the surface of MNP@MSNs-ACVA was carried out through amide bond formation between the carboxylic acid group of ACVA and the primary amine of AMA (Scheme S1). Typically, the carboxylic acid groups of MNP@MSNs-ACVA (20 mg) were activated by EDC (40 mg) and NHS (20 mg) in DMSO (4 mL). To crosslink ACVA to AMA, after 30 min activation at room temperature, 20 mg of AMA dissolved in DMSO (4 mL) was added to the activated MNP@MSNs-ACVA in DMSO and stirred for 24 h. Finally, AMA functionalized MNP@MSNs-ACVA (MNP@MSNs-AMA) was washed, centrifuged, and re-suspended in DMSO three times to remove the excess AMA, EDC, and NHS.

DOX loading in MNP@MSNs-AMA and *β*-CD capping

The loading of DOX was carried out by using water as the solvent. In general, 1 mg of MNP@MSNs-AMA was dispersed in deionized water (1 mL) with 3 mM DOX. After stirring for 24 h, 16 mg of the *β*-CD capping agent was added to the solution to prevent DOX from being released. The sample was designated as DOX-loaded MNP@MSNs-AMA-CD. After mixing for 48 h, the DOX-loaded MNP@MSNs-AMA-CD were centrifuged and washed with water seven times followed by PBS twice, to remove the excess DOX molecules. The final product was suspended in PBS or deionized water for further stimulated cargo release experiments.

Ultrasound-stimulated release of DOX by a probe sonicator

DOX-loaded MNP@MSNs-AMA-CD solution (0.75 mg/mL, 1 mL of PBS) was prepared in an Eppendorf tube. The tip of the probe sonicator (VCX 130, Sonics & Materials, Inc, Newtown, USA) was placed in the center of the solution. The ultrasound probe was set to a frequency of 20 kHz and output power of 21 W (power density: 75 W/cm^2). After various time durations of the ultrasound stimulation, the solution was centrifuged. The supernatant and pellet were collected separately for further quantification of DOX loading capacity and release efficiency by the plate reader (Tecan M1000).

MRI-guided high-intensity focused ultrasound (MRgHIFU)-stimulated release of DOX

All MRgHIFU experiments were conducted using a research HIFU system (Image Guided Therapy, Bordeaux, France) integrated with a whole-body 3 T MRI scanner (Prisma, Siemens Healthineers, Erlangen, Germany). The HIFU system had a 128-element annular transducer array with a diameter of 9 cm, frequency of 1 MHz, a focal point of 1 × 1 × 7 mm^3 in size, and a peak electrical power output of 1200 W. The electrical power output used ranged from 9 W to 290 W. DOX-loaded MNP@MSNs-AMA-CD solutions (0.15 mg/mL, 3 mL of PBS) were placed in sample wells (1.3 cm × 1.3 cm × 5 cm) in the agarose phantom (10 cm × 10 cm × 11.5 cm). The agarose phantom was placed on top of the HIFU transducer, which was secured on the patient table of the 3 T MRI scanner. Through both mechanical and electronic steering of the HIFU transducer, the focal point was placed at the center of the sample well. The samples were stimulated by HIFU at electrical power levels of 74 W (power density: 7400 W/cm^2) or 9 W (power density: 900 W/cm^2) for different durations (from 1 to 10 min). T_2 maps were acquired before and after the HIFU stimulation using a 2D turbo-spin-echo protocol (see the section T_2 mapping above) to compare the T_2 values. The subtracted T_2 maps were obtained by subtracting post-HIFU stimulation T_2 maps from pre-HIFU stimulation T_2 maps. The temperature of the solution during the HIFU stimulation was measured by a 2D single-slice gradient-echo MRI temperature mapping sequence with an image update rate of 1.8 seconds. To quantify the released amount of DOX, the HIFU-stimulated samples were removed from the phantom and spun down to separate the pellet and supernatant for fluorescence intensity measurement by the plate reader.

Loading capacity analysis of DOX

After being loaded with 3 mM DOX and capped with β-CD, DOX-loaded MNP@MSNs-AMA-CD was washed thoroughly with water seven times followed by PBS twice to remove the excess DOX. The DOX-loaded MNP@MSNs-AMA-CD solution (0.75 mg/mL, 1 mL of PBS) was put in a hot water bath at 80 °C for 30 min to completely release the loaded DOX in the nanoparticles. The released DOX was separated from MNP@MSNs-AMA-CD by centrifugation and recorded by the plate reader. The fluorescence intensity of the released DOX was integrated from 585 to 595 nm. As nearly 100% of the loaded DOX was released through this bulk heating treatment (80 °C for 30 min), the recorded fluorescence intensities indicated the total amount of loaded DOX in MNP@MSNs-AMA-CD. The loading capacity of DOX was then calculated following the definition of loading capacity: (mass of DOX loaded in pores/mass of nanoparticles) × 100%.

Release efficiency of DOX after ultrasound or HIFU stimulation

DOX-loaded MNP@MSNs-AMA-CD stimulated by ultrasound or HIFU was centrifuged to separate the pellet and the supernatant. The collected supernatants containing the released DOX were then analyzed by the plate reader. The fluorescence intensity of the released DOX was integrated from 585 to 595 nm. The fluorescence intensity corresponding to the DOX released

after being heated at 80°C for 30 min was designated as 100% release. The release efficiency of DOX was then calculated following the definition of release efficiency: (mass of released DOX/ mass of DOX loaded in pores) × 100%.

ζ-potential value measurement of MNP@MSNs-ACVA after heating or HIFU stimulation

0.75 mg of MNP@MSNs-ACVA was dispersed in 1 mL of water in an Eppendorf tube. For bulk heating treatment, the Eppendorf tubes containing the samples were put in a 37 or 80 °C hot water bath for 10 or 30 min, respectively. Afterwards, the solution was centrifuged and the nanoparticles were washed and redispersed in deionized water. For HIFU stimulation, the samples were stimulated with HIFU at a power of 74 W and a frequency of 1 MHz for 1, 5, or 10 min. Similarly, after the treatment, the solution was centrifuged and the nanoparticles were washed and redispersed in deionized water. Finally, the ζ-potential values of the samples after treatment were then measured.

***In vitro* cytotoxicity**

The viability of PANC-1 cells after the treatment of MNP@MSNs-AMA-CD or DOX-loaded MNP@MSNs-AMA-CD were examined by using a cell counting kit-8 (CCK-8) assay. The cells were seeded in 96-well plates at a density of 5 x 10^3 cells per well in 200 μL of DMEM supplemented with 10% FBS and 1% antibiotics in a humidity-controlled incubator at 37 °C for 24 h attachment. After the attachment, the medium was removed and the cells were treated with 0, 10, 25, 50, 75, 100, 200, and 300 μg/mL MNP@MSNs-AMA-CD for 4, 24, 48, or 72 h, or 0, 10, 25, 50, 75, 100, and 200 μg/mL DOX-loaded MNP@MSNs-AMA-CD for 4 h in 200 μL of fresh DMEM in an incubator at 37 °C. After incubation, the medium was removed and the nanoparticle-treated cells were washed twice with DPBS. To measure the cell viability, DMEM (100 μL) and CCK-8 cellular cytotoxicity reagent (10 μL) were added to the cells in each well and incubated for 2 h at 37 °C. The number of viable cells was determined by using the plate reader (Tecan M1000) to measure the absorbance at 450 nm and 650 nm (as the reference). DMEM (100 μL) containing the CCK-8 reagent (10 μL) served as a background. For the cell proliferation study, after 4 h treatment of 0, 10, 25, 50, 75, 100, and 200 μg/mL DOX-loaded MNP@MSNs-AMA-CD, the medium was removed and the nanoparticle-treated cells were washed twice with DPBS. The cells were allowed to grow in a fresh culture medium for another 18 h and the cell viability was determined by the CCK-8 assay as above.

***In vitro* MRgHIFU-stimulated DOX release and cellular T_2 monitoring**

PANC-1 cells were seeded in 24-well plates at a density of 10^5 cells per well in 500 μL of DMEM supplemented with 10% FBS and 1% antibiotics in a humidity-controlled incubator at 37 °C for 24 h attachment. After the attachment, the medium was removed and the cells were treated with DOX-loaded MNP@MSNs-AMA-CD (200 μg/mL) in 300 μL of fresh DMEM in an incubator at 37 °C. The control groups including cells only (negative control), cells treated with an equivalent amount of free DOX (positive control) to the DOX-loaded MNP@MSNs-AMA-CD, and cells treated with MNP@MSNs-AMA-CD (200 μg/mL) were also investigated. After 4 h incubation, the medium was removed and the cells were washed twice with DPBS (500 μL × 2). The cells were harvested by trypsinization with 0.05% trypsin-EDTA and suspended in DMEM. The cell suspensions were then transferred into 15 mL Falcon plastic tubes in preparation for MRgHIFU experiments. The research HIFU system (Image Guided Therapy, Bordeaux, France) integrated with the whole-body 3 T MRI scanner (Prisma, Siemens Healthineers, Erlangen, Germany) was

used. To stimulate the release of DOX in cells by MRgHIFU, the cell suspensions were transferred into sample wells (1.3 cm × 1.3 cm × 5 cm) in the agarose phantom (10 cm × 10 cm × 11.5 cm). The agarose phantom was placed on top of the HIFU transducer, which was secured on the patient table of the 3 T MRI scanner. The HIFU focal point was placed at the center of the sample well and the cells were stimulated by HIFU at an electrical power level of 9 W (power density: 900 W/cm^2) for different durations (0, 1, 2, or 5 min). MRI T_2 mapping was performed before and after the HIFU stimulation using a 2D TSE protocol (see the section T_2 mapping above) to compare the T_2 values. The temperature of the sample during the HIFU stimulation was measured by a 2D single-slice gradient-echo MRI temperature mapping sequence with an image update rate of 1.8 seconds. After the HIFU stimulation and T_2 mapping, the treated cells were allowed to grow and attach in 96-well plates in 200 μL of DMEM supplemented with 10% FBS and 1% antibiotics in a humidity-controlled incubator at 37 °C for 18 h. The cell viability after the HIFU stimulation was measured by the CCK-8 assay. Basically, after removing the medium, DMEM (100 μL) and CCK-8 reagent (10 μL) were added to the cells in each well and incubated for 2 h at 37 °C. The number of viable cells was determined by using the plate reader (Tecan M1000) to measure the absorbance at 450 nm and 650 nm (as the reference). DMEM (100 μL) containing the CCK-8 reagent (10 μL) served as a background.

Fluorescence microscope images of PANC-1 cells after HIFU stimulations

After the HIFU stimulation and T_2 mapping, the PANC-1 cells treated with DOX-loaded MNP@MSNs-AMA-CD (200 μg/mL) were allowed to grow and attach in 8-well chamber slides at a density of 2.5×10^4 cells per well in 500 μL of DMEM supplemented with 10% FBS and 1% antibiotics in a humidity-controlled incubator at 37 °C. After 18 h attachment, the cells were washed with DPBS three times (500 μL × 3) followed by fixing with 4 % paraformaldehyde in PBS for 20 min. The fixed cells were then washed with DPBS three times (500 μL × 3). Afterwards, the cell nuclei were stained with Hoechst 33342 (500 μL, 5 μg/mL) for 20 min followed by washing with DPBS five times (500 μL × 5). The stained cells were covered by mounting medium cover glass before taking fluorescence images using a Zeiss fluorescence microscope.

III. Supporting scheme

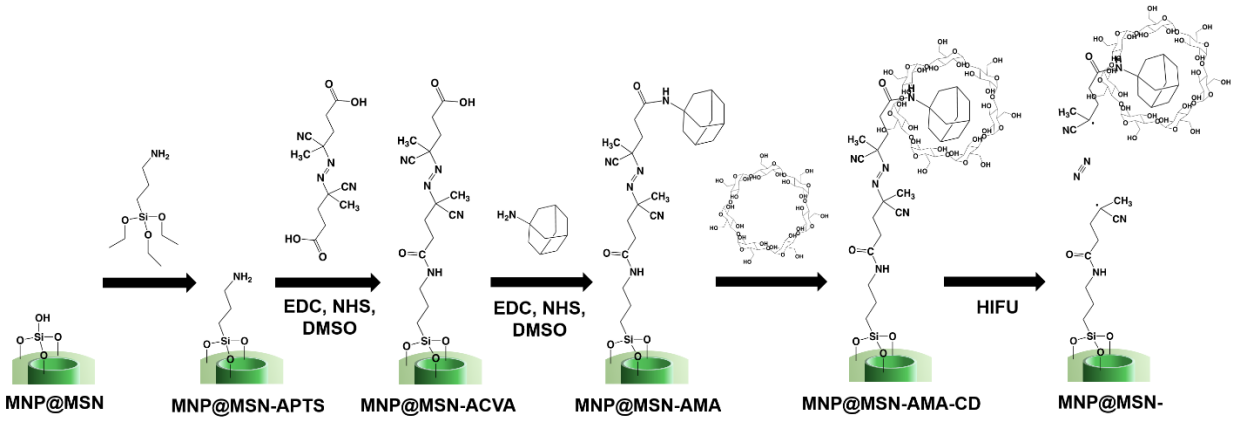

Scheme S1. Synthesis of HIFU-responsive cap on the surface of MNP@MSN. Followed by the APTS modification, ACVA, AMA, and β-CD are conjugated sequentially on the surface of core@shell nanoparticles (EDC, 1-ethyl-3-(3-dimethylaminopropyl) carbodiimide; NHS, N-hydroxysuccinimide; DMSO, dimethyl sulfoxide). After stimulation by HIFU, the cleavage of the C−N bonds of ACVA makes the bulky β-CD and AMA complexation leave from the surface, and thus releases the cargo from the nanoparticles.

IV. Supporting figures and discussion

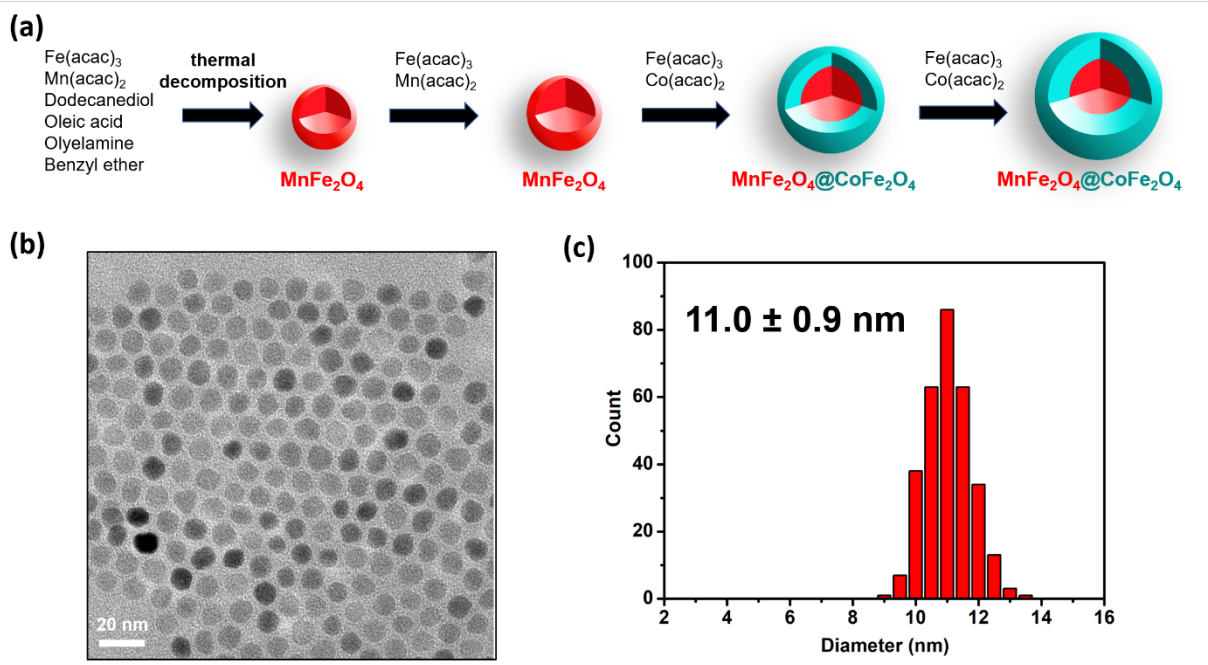

Figure S1. (a) Schematic illustration of the synthesis of $MnFe_2O_4$@$CoFe_2O_4$ nanoparticles (MNPs) by a seed-mediated thermal decomposition method. (b) The TEM image and (c) diameter distribution of the final $MnFe_2O_4$@$CoFe_2O_4$ nanoparticles.

Discussion of Figure S1

$MnFe_2O_4$@$CoFe_2O_4$ nanoparticles has an uniform size distribution of 11.0 ± 0.9 nm.

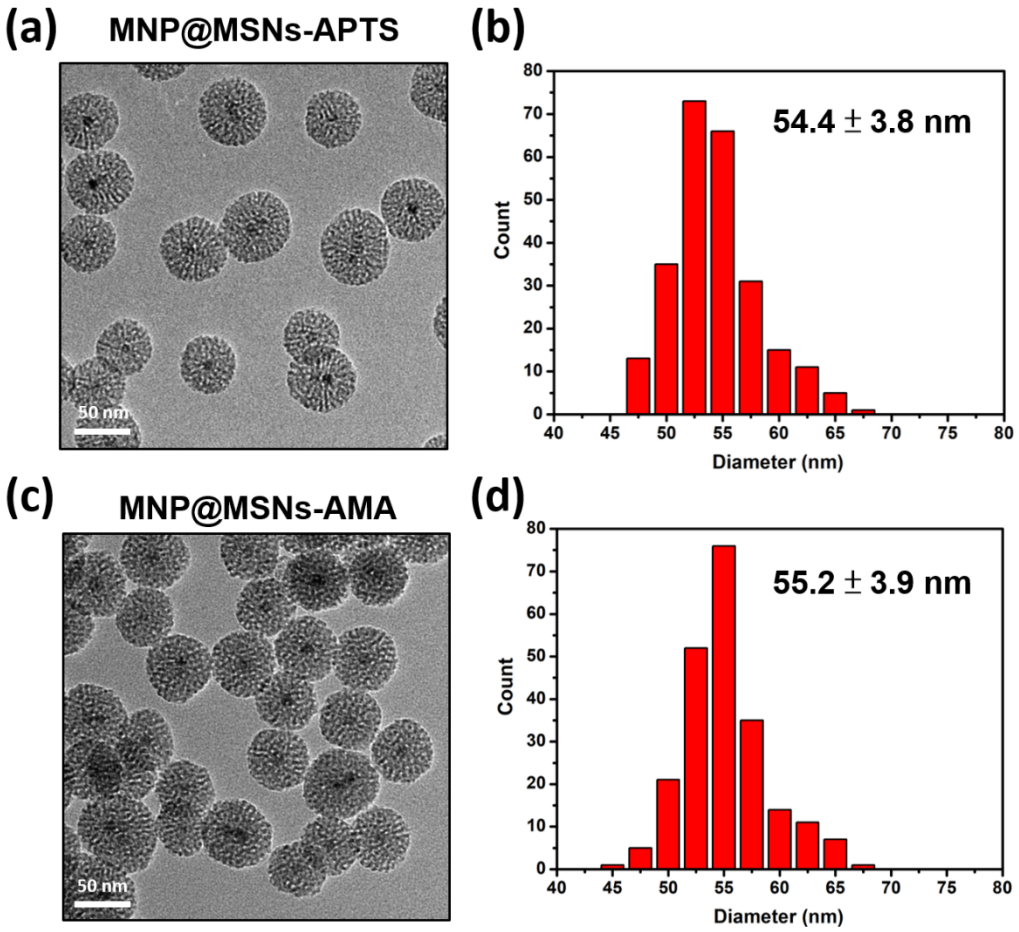

Figure S2. (a) The TEM image and (b) size distribution of 54.4 nm MNP@MSNs-APTS. (c) The TEM image and (d) size distribution of 55.2 nm MNP@MSNs-AMA.

Discussion of Figure S2

MNP@MSNs-AMA is 55.2 nm in size with obvious mesoporous structure, very similar to that of MNP@MSNs-APTS (55.4 nm), indicating that the particles were not damaged after the surface functionalization and had uniform size distributions.

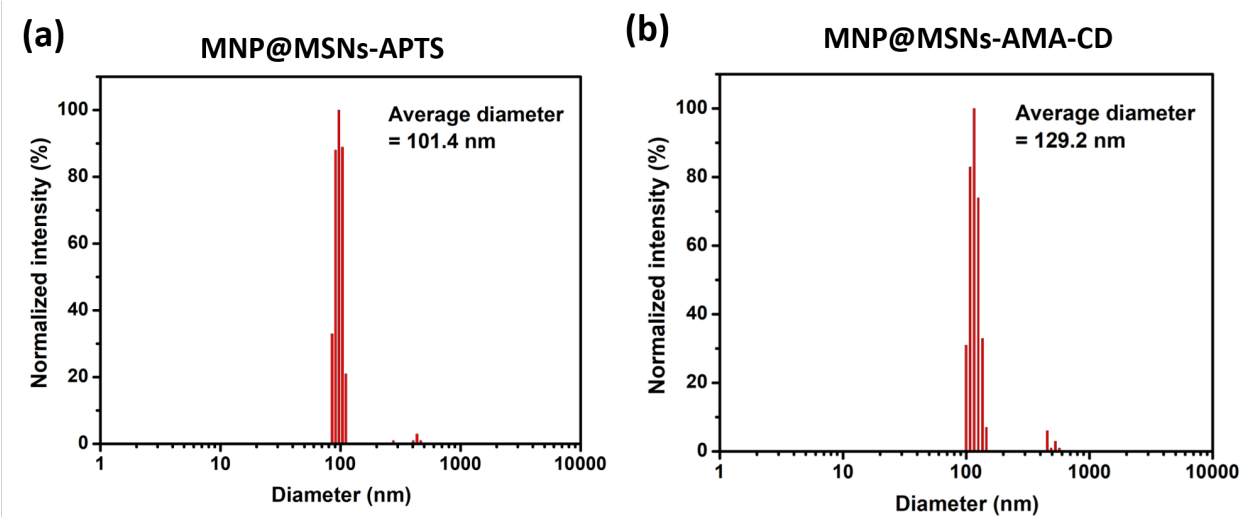

Figure S3. Dynamic light scattering diameter distribution of MNP@MSNs-APTS (a) and MNP@MSNs-AMA-CD (b) in deionized water at room temperature.

Discussion of Figure S3

The particles with the bulky hydrophilic β-CD caps retained the good water dispersibility of MNP@MSNs-AMA-CD and had an increased hydrodynamic diameter of 129.2 nm.

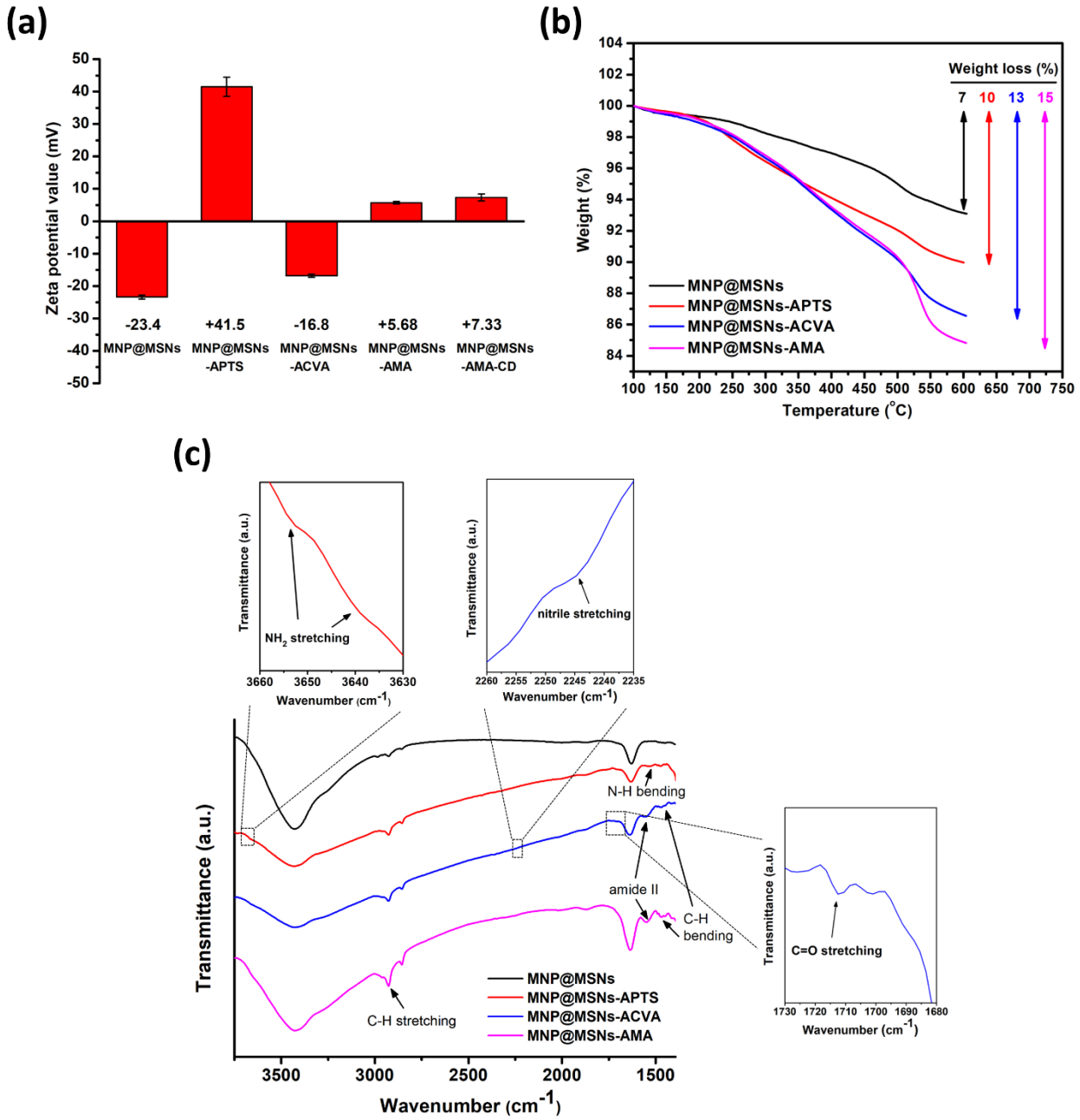

Figure S4. (a) ζ-potential values, (b) thermogravimetric analysis, and (c) Fourier-transform infrared spectroscopy of MNP@MSNs, MNP@ MSNs-APTS, MNP@MSNs-ACVA, and MNP@MSNs-AMA. ζ-potential value of MNP@MSNs-AMA-CD is also shown in (a).

Discussion of Figure S4

The ζ-potential value of MNP@MSNs-APTS was +41.5 mV, much more positive than that of MNP@MSNs (-23.4 mV), showing abundant primary amines on the surface of MNP@MSNs-APTS. MNP@MSNs-ACVA has a negative ζ-potential value of -16.8 mV. This significant decrease in the ζ-potential value indicates that ACVA molecules with carboxylates on both ends were successfully attached to the surface of MNP@MSNs-APTS, with one end stretching out from the surface of MNP@MSNs-ACVA available for further AMA conjugation. MNP@MSNs-AMA

with the nearly neutral ζ-potential value of +5.68 mV confirms the conjugation of the amine on AMA to the free carboxylate on the surface of MNP@MSNs-ACVA, leaving the uncharged functional group on AMA stretching out from the surface of the particles (Scheme S1). By TGA, the weight loss of MNP@MSNs, MNP@MSNs-APTS, MNP@MSNs-ACVA, and MNP@MSNs-AMA were 7 %, 10 %, 13 %, and 15 %, respectively, confirming the presence of organic matters were 3 % (APTS), 3 % (ACVA), and 2 % (AMA), respectively. FT-IR spectroscopy was analyzed after each conjugation step. The appearance of two bands in the IR spectrum of MNP@MSNs-APTS due to N-H stretching vibrations at $\nu =$ 3640 cm^{-1} and $\nu =$ 3652 cm^{-1} and one peak at $\nu =$ 1531 cm^{-1} due to N-H bending show the presence of primary amines attached to the surface of MNP@MSNs-APTS. The successful conjugation of ACVA to the surface of MNP@MSNs-APTS through secondary amide bond formation was confirmed by a new characteristic amide absorption (amide II) at $\nu =$ 1550 cm^{-1}. A nitrile absorption from ACVA at $\nu =$ 2245 cm^{-1} (nitrile stretching) and newly emerging absorptions at $\nu =$ 1712 cm^{-1} (C=O stretching) and $\nu =$ 1447 cm^{-1} (C-H bending) also support the successful ACVA conjugation on MNP@MSNs-APTS. Finally, the conjugation of AMA on the surface of MNP@MSNs-ACVA is confirmed by the appearance of the absorption at $\nu =$ 1469 cm^{-1} (C-H bending) and two absorption peaks at $\nu =$ 2856 cm^{-1} and $\nu =$ 2927 cm^{-1} (C-H stretching) from AMA.

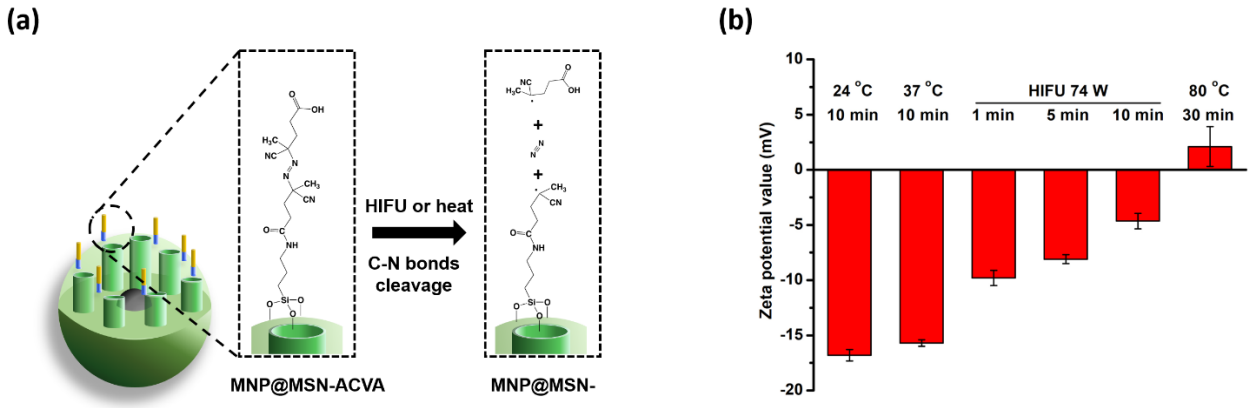

Figure S5. (a) Cleavage of C−N bonds caused by HIFU simulation or bulk heating. (b) ζ-potential values of MNP@MSNs-ACVA in deionized water after HIFU stimulation (74 W) for 1, 5, or 10 min, or bulk heating in a 37 or 80 °C water bath for 10 or 30 min, respectively. MNP@MSNs-ACVA immersed in a water bath at room temperature (24 °C) for 10 min was recorded as a control. The concentration of MNP@MSNs-ACVA in deionized water is 0.5 mg/mL.

Discussion of Figure S5

The ACVA gatekeeper was stable on the nanoparticle's surface at physiological temperature (37 °C) as revealed by the similar negative ζ-potential value compared to that at room temperature (24 °C). On the other hand, the cleavage of ACVA occurred when the nanoparticles were heated at 80 °C for 30 min, leaving fewer carboxylic acid end groups on the nanoparticle's surface, and thus a neutral or positive charge was observed. The gradual increase of the nanoparticle's charge after HIFU stimulation corroborated the HIFU-induced ACVA cleavage.

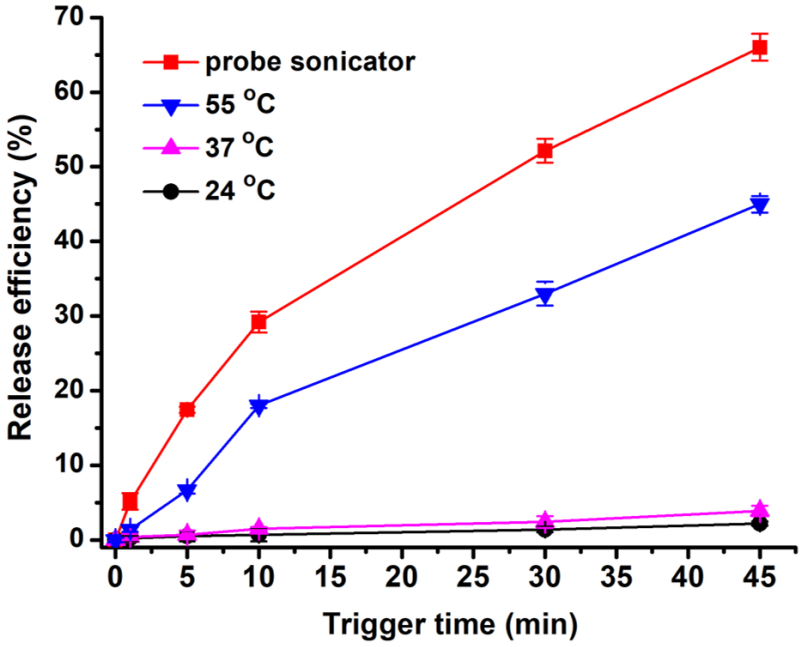

Figure S6. Ultrasound-stimulated DOX release using a probe sonicator. Time-dependent release profile of DOX from MNP@MSNs-AMA-CD after probe sonication (red) or immersed in a 24 °C (black), 37 °C (pink), or 55 °C (blue) water bath. The loading capacity of DOX in MNP@MSNs-AMA-CD was 3.6 ± 0.6%.

Discussion of Figure S6

Ultrasound-responsiveness of the cap was first tested using a probe sonicator. The resulting DOX release from the uncapped pores was determined by fluorescence spectroscopy and quantified as DOX release efficiency, defined as (mass of released DOX/mass of DOX loaded in pores) × 100%. DOX release efficiency increased as the ultrasound trigger time increased. The release rate exhibited two phases consisting of an initial fast release and ensuing slower release. The temperature of the solution after 45 min of probe ultrasonication increased to 55 °C from room temperature of 24 °C. Interestingly, the amount of DOX released stimulated solely by heating at 55 °C was lower than that released by ultrasound, implying that the mechanical effects of ultrasound (*e.g.*, cavitation) play a role in inducing more ACVA cleavage and/or greater DOX diffusion.

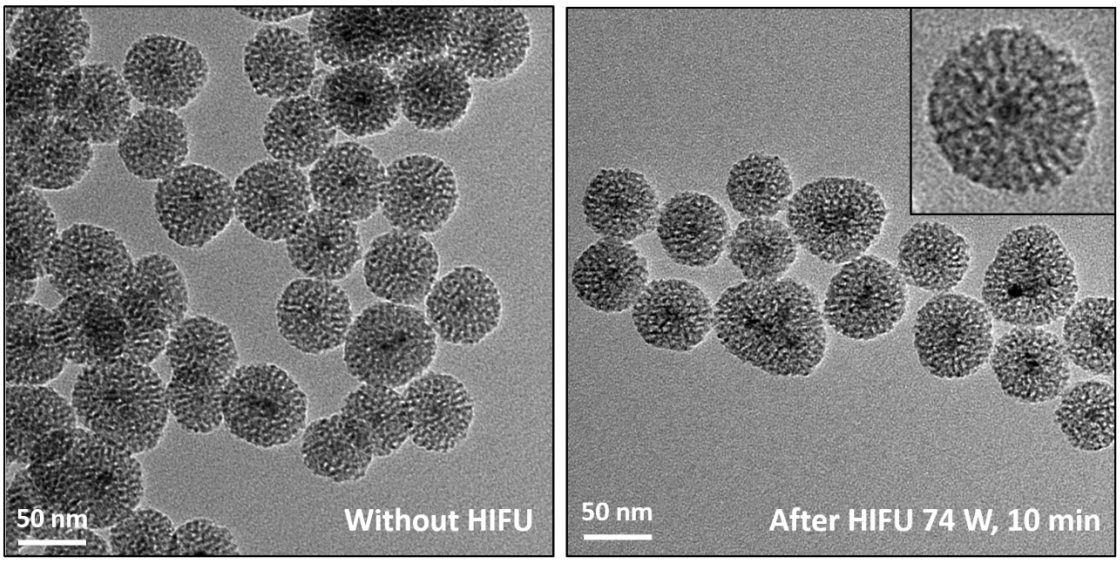

Figure S7. TEM images of MNP@MSN-AMA with and without 10 min of HIFU stimulation (74 W).

Discussion of Figure S7

TEM images showed that the morphology and pore structure of the HIFU-stimulated nanoparticles remained intact.

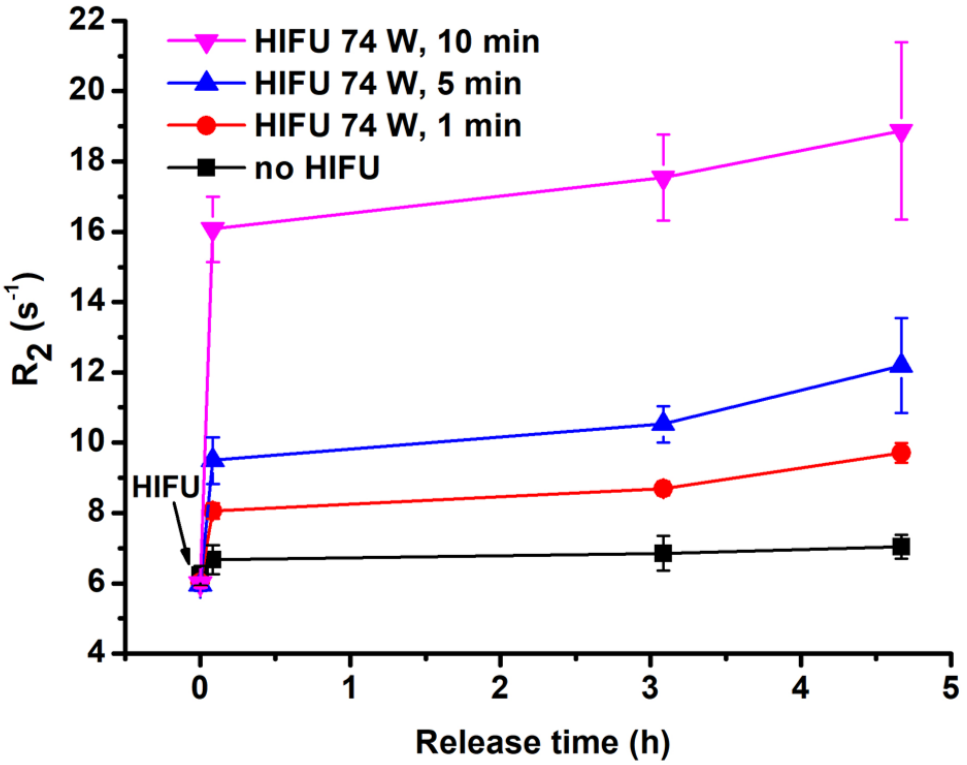

Figure S8. Long-term R_2 monitoring with different HIFU stimulation times until 4.75 h after each HIFU stimulation.

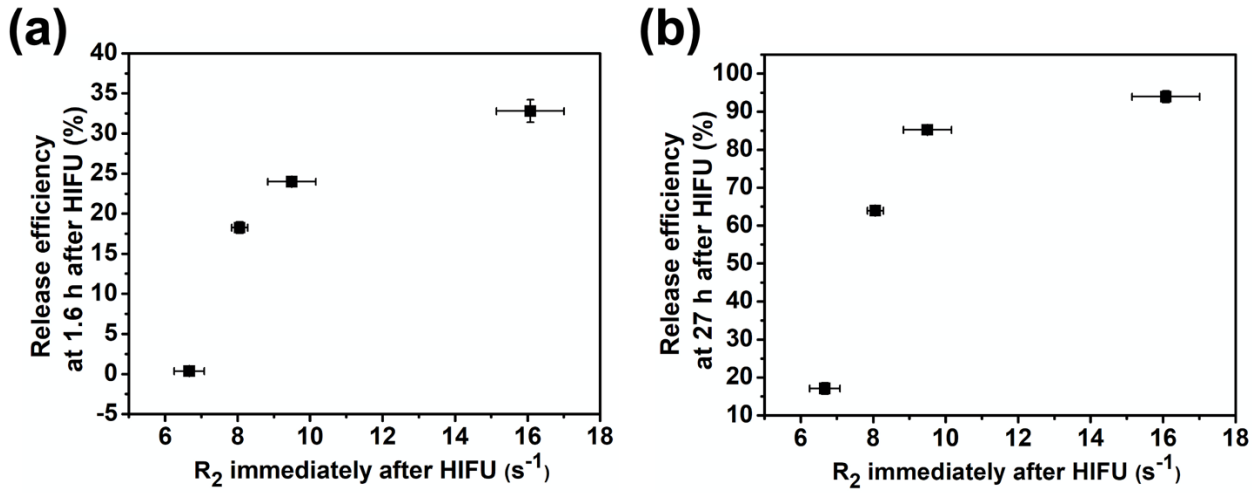

Figure S9. Associations between release efficiencies of DOX measured at 1.6 and 27 h after HIFU stimulations and R_2 quantified immediately after HIFU stimulations were shown in (a) and (b), respectively. The release efficiencies of DOX were obtained from Fig. 2b and the R_2 values were obtained from Fig. 3a.

Discussion of Figure S9

DOX release efficiencies measured at 1.6 and 27 h after HIFU stimulation (Fig. 2b) showed associations with R_2, indicating that the release of DOX can be predicted by using this DOX release versus R_2 plot. For example, from the observed change in R_2 value from 6.7 s^{-1} before HIFU-stimulated release to 16 s^{-1} after release, we may predict that there will be around 33% and 94% of released DOX at 1.6 and 27 h after HIFU stimulation, respectively.

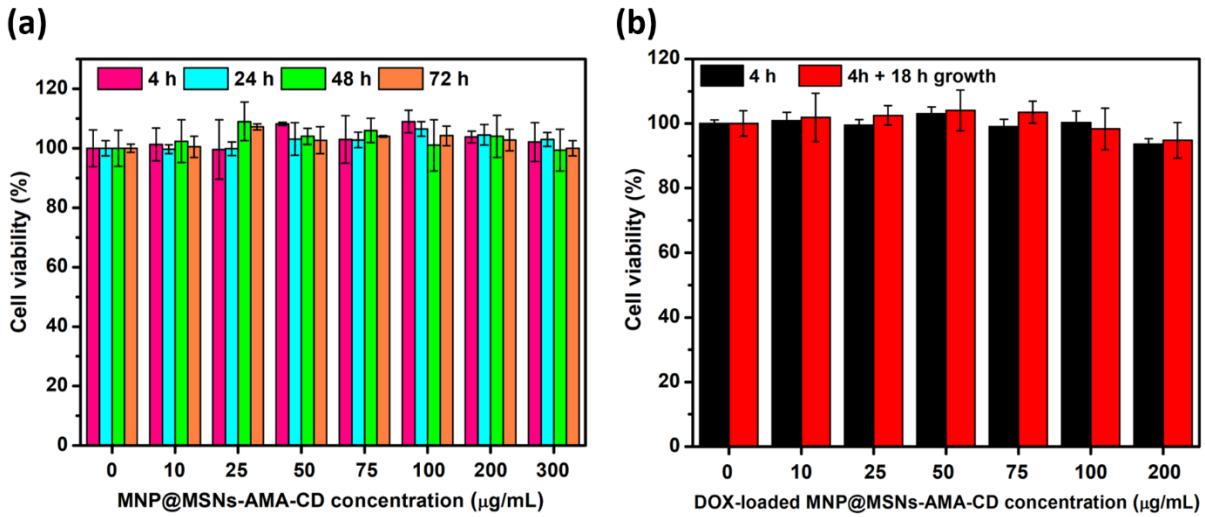

Figure S10. (a) Cytotoxicity of MNP@MSNs-AMA-CD. PANC-1 cells were incubated with MNP@MSNs-AMA-CD at various nanoparticle concentrations for 4, 24, 48, and 72 h, and the viability was determined by a CCK-8 assay and normalized to the cells without MNP@MSNs-AMA-CD treatment (control). Data are displayed as the mean (color bar) ± standard deviation (SD) (black brackets) of three independent experiments. (b) Cytotoxicity of DOX-loaded MNP@MSNs-AMA-CD. PANC-1 was incubated with DOX-loaded MNP@MSNs-AMA-CD at various concentrations for 4 h. The viability was determined by the CCK-8 assay and normalized to the cells without DOX-loaded MNP@MSNs-AMA-CD treatment (control). After the 4 h treatment of DOX-loaded MNP@MSNs-AMA-CD, the cells were allowed to grow in the regular culture medium for 18 h, and the viability was determined by the CCK-8 assay and normalized to the control. Data are displayed as the mean (color bar) ± SD (black brackets) of three independent experiments.

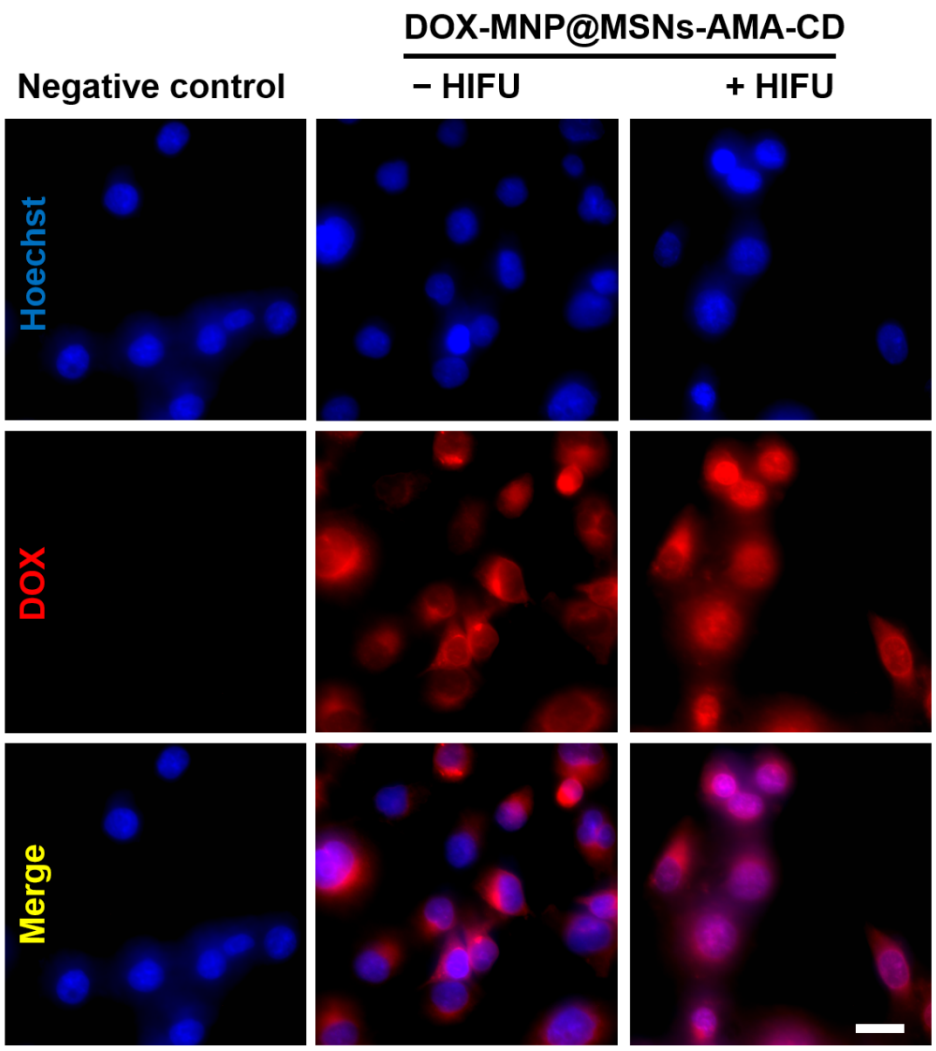

Figure S11. Fluorescence microscope images of PANC-1 cells after 4 h of treatment with DOX-loaded MNP@MSNs-AMA-CD with and without the following 2 min of HIFU stimulation (9 W). The negative control group is cells without the treatment with DOX-loaded MNP@MSNs-AMA-CD. Panels from top to bottom: blue-colored fluorescence from nucleus of PANC-1 cells stained by Hoechst 33342, red-colored fluorescence from DOX, and the merged images from two channels. The scale bar is 20 μm.

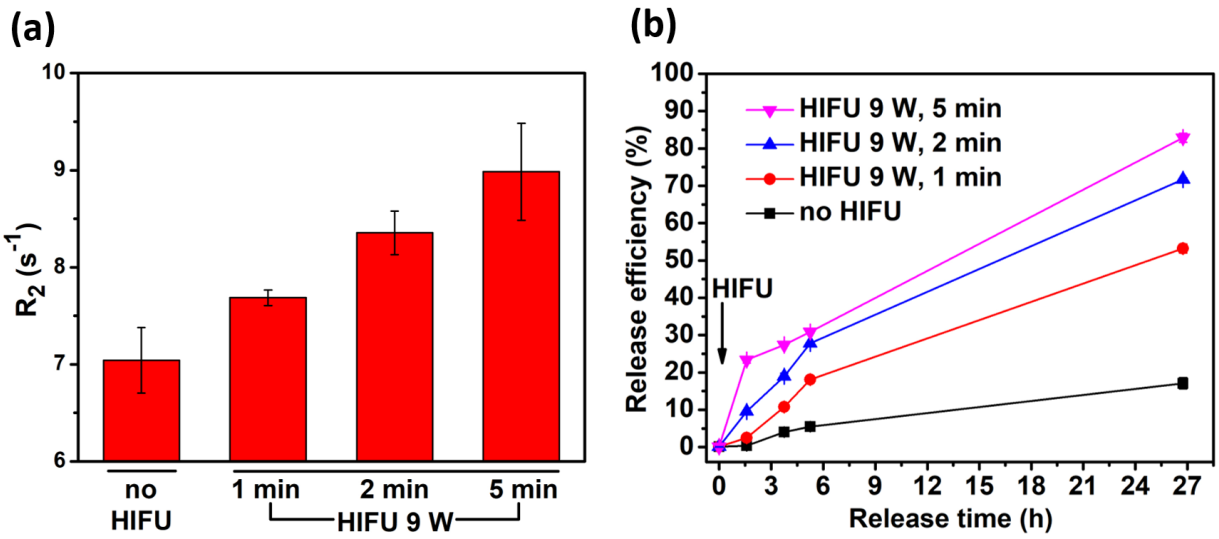

Figure S12. (a) Time-dependent release profile of DOX over a period of 27 h after 1, 5, or 10 min of HIFU stimulation (1 MHz, 9 W) and (b) R_2 measured immediately after those HIFU stimulations.

Discussion of Figure S12

The capability of these conservative HIFU parameters to stimulate DOX release and change R_2 was confirmed by the familiar biphasic DOX release profile and R_2 as a function of HIFU stimulation times in solution. No increase in bulk temperature was observed after 1 and 2 min of HIFU stimulations, with only 2 °C increase after 5 min of HIFU stimulation, from room temperature of 24 °C.

V. Supplementary notes

Note S1: Methods for T_2 fitting

The standard Carr-Purcell-Meiboom-Gill (CPMG) signal model was used to calculate T_2 maps, where images acquired with different echo times (TEs) were fit pixel-wise to the equation $\boxed{M = M_0 e^{-\tau/T_2}}$, with M_0 being the magnetization at thermal equilibrium, M being the signal intensity of images acquired at TE = $\boxed{\tau}$.

VI. References

[1] J. T. de Bever, H. Odéen, L. W. Hofstetter and D. L. Parker, *Magn. Reson. Med*., **2018**, *79*, 1515–1524.

[2] A. I. Farrer, H. Odéen, J. T. de Bever, B. Coats, D. L. Parker, A. Payne and D. A. Christensen, *J. Ther. Ultrasound*, **2015**, *3*, 9.

[3] W. Chen, C. A. Cheng, J. I. Zink, *ACS Nano* **2019**, *13*, 1292−1308.

[4] W. Chen, F. Lu, C. C. V. Chen, K. C. Mo, Y. Hung, Z. X. Guo, C. H. Lin, M. H. Lin, Y. H. Lin, C. Chang, C. Y. Mou, *NMR Biomed.* **2013**, *26*, 1176−1185.